Low temperature metal-organic chemical vapor deposition of tungsten nitride as diffusion barrier for copper metallization

Jean E. Kelsey, Cindy Goldberg, Guillermo Nuesca, Gregory Peterson, and Alain E. Kaloyeros[a)]
Center for Advanced Thin Film Technology and Department of Physics, The University at Albany—SUNY, Albany, New York 12222

Barry Arkles
Gelest Inc., Tullytown, Pennsylvania 19007

(Received 15 January 1999; accepted 12 February 1999)

A metal-organic chemical vapor deposition process has been developed for the growth of amorphous tungsten nitride thin films for barrier layer applications in ultralarge scale integration copper interconnect schemes. The process employs tungsten hexacarbonyl, [$W(CO)_6$] and ammonia (NH_3) as, respectively, the tungsten and nitrogen sources. Tungsten nitride films were produced within a wide process window, including a substrate temperature of 200–350 °C, $W(CO)_6$ flow rate of 1–20 sccm, reactor pressure of 0.2–0.5 Torr, and NH_3 flow rates of 100–500 sccm. The films were analyzed by x-ray photoelectron spectroscopy, cross-section scanning electron microscopy, x-ray diffraction, transmission electron microscopy, four-point resistivity probe, and Rutherford backscattering spectrometry. These studies indicated that the films consisted predominantly of a W_2N phase. Films were grown with carbon and oxygen concentrations $\leq$5 at. %, even at the lowest processing temperature investigated, where precursor dissociation would be expected to be the least efficient given the reduced thermal budget available to the decomposition reaction. Films deposited below 275 °C were amorphous, while those deposited between 275 and 350 °C were polycrystalline. Resistivities as low as 123 $\mu\Omega$ cm were achieved for 50-nm-thick films, with corresponding step coverage better than 90% in nominal 0.25 μm trench structures with aspect ratio of 4:1.

As computer chip device dimensions continue their evolution towards feature sizes below 100 nm, new liner materials and associated process technologies are needed to ensure viable diffusion barrier/adhesion promoter performance between the conductor and the surrounding regions of silicon- and dielectric-based materials. These liners must possess mechanical and structural integrity, good conformality within aggressive device features, high conductivity to minimize plug overall effective resistance, and thermal, mechanical, and electrical compatibility with neighboring conductor and dielectric material systems. Most importantly, liner materials are expected to meet these stringent requirements at increasingly reduced thickness, in order to maximize the real estate available for the primary metal conductor within the continuously decreasing device dimensions. In particular, liner thickness is predicted to decrease from 20 nm for the 0.15 μm device generation, to less than 6 nm for its 0.05 μm counterpart.[1]

These needs are further complicated by the on-going transition from aluminum- to copper-based metallization schemes, and which required exploring new candidate liner material that are chemically and thermodynamically more stable towards copper diffusion and migration than the presently used titanium/titanium nitride materials. These include binary compounds, such as tantalum nitride (TaN_x) and tungsten nitride (WN_x),[2,3] and ternary compounds such as tantalum-silicon-nitride ($TaSi_xN_y$) and tungsten-silicon-nitride (WSi_xN_y).[4]

In this respect, WN_x presents a potentially viable solution given its attractive properties as highly refractory material with excellent mechanical and chemical properties. Additionally, it can be deposited in amorphous form.[5] This feature is highly desirable given that an amorphous film inherently has no grain boundaries, therefore providing added stability towards metal migration by eliminating grain boundaries as a primary path for metal diffusion. Accordingly, prior work in the literature has successfully demonstrated the applicability of W_2N as effective barrier against Cu diffusion at temperatures as high as 750 °C.[3]

WN_x has already been deposited by reactive sputtering,[3] chemical vapor deposition (CVD) from tungsten hexafluoride (WF_6) and ammonia (NH_3),[6] and metal-organic CVD (MOCVD) from the single W source bis-tert-butylimido)bis(terbtylamido)tungsten [$(^tBuN)_2W(NH^tBu)_2$].[7] Unfortunately, the application of sputtering techniques is limited by concerns over their ability to provide good conformality in sub-100 nm device structures. Optimized CVD-based methods, on the other hand, could provide viable step coverage in such aggressive topographies, thus allowing the potential use of the same CVD liner technology in multiple generations of sub-100 nm microprocessor and memory products. In this respect, inorganic CVD from WF_6 and NH_3 could pose some challenges due to: (a) transport and handling concerns attributed to the high reactivity of the fluori-

a)Corresponding author; electronic mail: ak127@csc.albany.edu

nated WF_6 source, (b) process concerns caused by potential gas phase particle generation in the reaction of WF_6 and NH_3, and (c) reliability issues pertaining to the possible inclusion of fluorine, a fast diffuser in Cu, in the resulting WN_x liner. MOCVD from single source precursors, on the other hand, has typically required high processing temperatures, in excess of 450 °C, and resulted in film resistivity greater than 620 $\mu\Omega$ cm.[7]

In view of these considerations, work by the present investigators has explored the nonfluorinated alternative tungsten hexacarbonyl, $W(CO)_6$. $W(CO)_6$ is a white solid with high vapor pressure, namely, 2 Torr at 35 °C, and a relatively low melting point of 150 °C. More importantly, it is characterized by a coordinative covalent bond between W and CO, with W and CO formally in the zero oxidation state. As such, the dissociation energy of W–CO bonds is relatively low, with recombination being easily interrupted by the presence of nitrogen-bearing reactants, such as ammonia, leading to the formation of tungsten nitride at low temperature.

Process development was implemented in an alpha-type, 200 mm wafer, cold-wall, plasma-capable CVD reactor, equipped with a high vacuum loadlock for wafer transport and handling. The use of the loadlock system allowed tight control over the cleanliness of the CVD chamber, and prevented undesirable contamination from exposure to ambient conditions during sample loading and unloading. In addition, a cryogenic pump was employed to routinely achieve a chamber base pressure in the 10^{-6} Torr, while a roots blower pumping stack was used during actual growth runs. The precursor was placed in a reservoir heated to temperatures ranging from 85 to 110 °C, depending on the processing conditions, and its flow into the reactor was regulated by an MKS 1153 solid source delivery system (SSDS). The SSDS and all delivery lines were heated to 120 °C to prevent precursor recondensation.

The parallel-plate, radio-frequency plasma (18.56 MHz) capability was employed for *in situ*, predeposition, wafer clean in a hydrogen–argon mixture plasma prior to the actual deposition step. In this parallel plate configuration, the wafer was loaded onto the lower, heated, electrode. Once the predeposition cleaning step was completed, precursor vapor was premixed with hydrogen (H_2) at the reactor inlet, then introduced into the reactor chamber through a cone-shaped showerhead. The cone was designed for uniform distribution of reactant vapor across the entire surface area of the 200 mm wafer. Conversely, NH_3 was introduced directly into the chamber through a separate feedthrough. The use of a separate inlet for NH_3 was designed to eliminate any early contact with the precursor vapor, which could lead to premature reaction and precursor decomposition. The deposition of tungsten nitride was investigated within the process window presented in Table I.

The structural, compositional, and electrical properties of the tungsten nitride films thus produced were analyzed by x-ray photoelectron spectroscopy (XPS), cross-section scanning electron microscopy (CS–SEM), x-ray diffraction (XRD), transmission electron microscopy (TEM), four-point resistivity probe, and Rutherford backscattering spectrometry (RBS).

TABLE I. Process window investigated for the deposition of tungsten nitride films.

Parameter	Value
$W(CO)_6$ source temperature	85–110 °C
Wafer temperature	200–350 °C
Reactor base pressure	$\sim 10^{-6}$ Torr
Reactor process pressure	0.2–0.5 Torr
Precursor flow rate	1–20 sccm
Hydrogen flow rate	50–200 sccm
Ammonia flow rate	100–500 sccm
Growth rate	4–10 nm/min

XPS studies were performed with a Perkin–Elmer Physical Electronics Model 5600 multitechnique system with a spherical capacitor analyzer. The analyzer was calibrated using the gold $f_{7/2}$ line at 83.8 eV as a reference line. All spectra were acquired using a pass energy of 58.7 eV at a resolution of 0.25 eV. The primary x-ray beam employed was Mg $K\alpha$ at 1274 eV, with primary beam energy and power of, respectively, 15 keV and 300 W. The results were standardized with a pure W film sputtered on a S substrate since a W_2N standard was not available.

XPS results indicated that at the lowest processing temperature investigated, where precursor dissociation would be expected to be the least efficient given the reduced thermal budget available to the decomposition reaction, films were grown with carbon and oxygen concentrations $\leq$5 at. %. In addition, XPS indicated a constant N/W ratio throughout the bulk of the tungsten nitride film. Additionally, high resolution XPS elemental core peak analysis was performed to determine the exact nature of the tungsten nitride phase produced. In this respect, Figs. 1(a) and 1(b) compare peak profile and associated binding energy location for the XPS W $4f$ core peaks from, respectively, a sputter-deposited W standard and a typical MOCVD WN_x sample. For both samples, binding energy locations were calibrated using the energy location of the corresponding surface hydrocarbon peak as reference. A shift of $\sim$1 eV towards higher binding energy was observed for the W $4f_{7/2}$ peak in the MOCVD WN_x sample in comparison with its counterpart in pure W. This

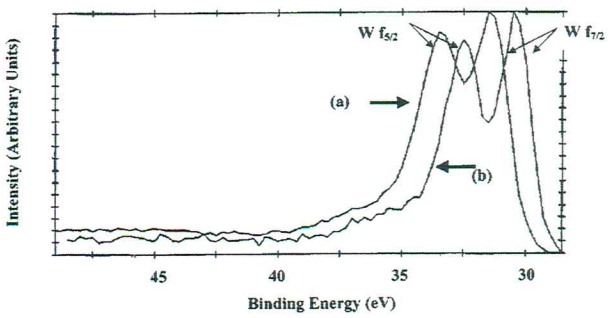

FIG. 1. High resolution XPS spectra of the W $4f$ elemental core peaks for: (a) MOCVD W_2N from $W(CO)_6$ and (b) sputtered pure W standard.

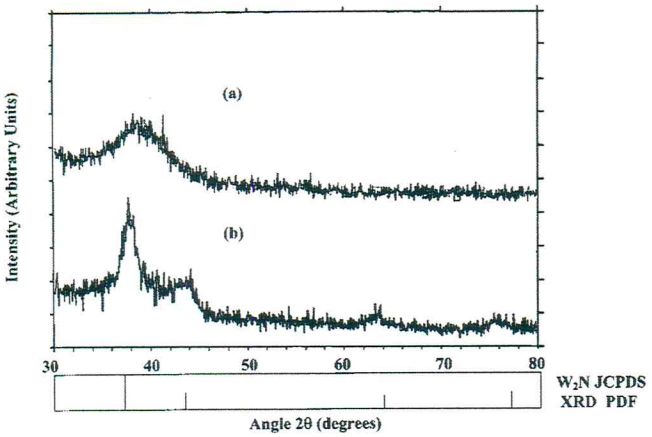

FIG. 2. XRD scans of MOCVD W_2N films grown from $W(CO)_6$ at substrate temperatures of: (a) 200 °C (film thickness ~52 nm) and (b) 275 °C (film thickness ~63 nm).

shift is in agreement with the findings of Takeyama and Noya, and indicates the formation of a W_2N phase.[8]

XRD analyses were carried out on a Scintag XDS 2000 x-ray diffractometer equipped with a Cu $K\alpha$ x-ray source and a horizontal wide angle four axis goniometer with stepping motors which allowed independent or coupled theta/2 theta axes motion. XRD spectra were collected in the low angle incidence geometry, with an angle of incidence of 5° being used (angle as measured between the incident beam and the sample surface). In this mode, data collection is performed by fixing the incidence angle at 5°, and the XRD pattern is collected for 2θ ranging from 30° to 80°. The collected XRD patterns were compared to tungsten nitride reference patterns from the standard Joint Committee for Powder Diffraction Standards (JCPDS) powder diffraction file (PDF). In this respect, XRD indicated a completely amorphous phase for films grown at substrate temperatures below

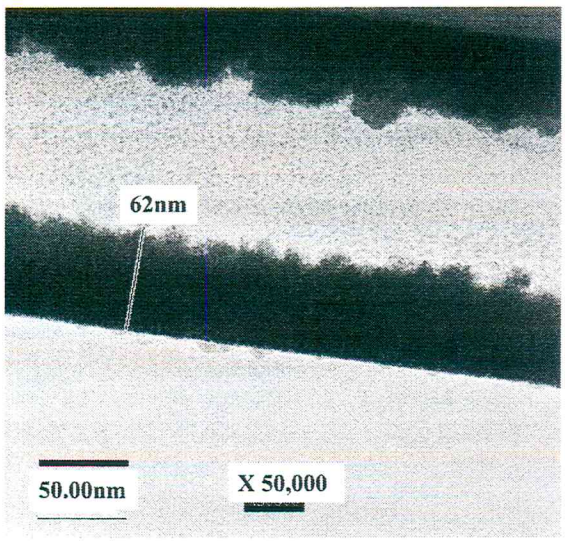

FIG. 3. Bright field cross-section TEM of a 62-nm-thick MOCVD-grown W_2N.

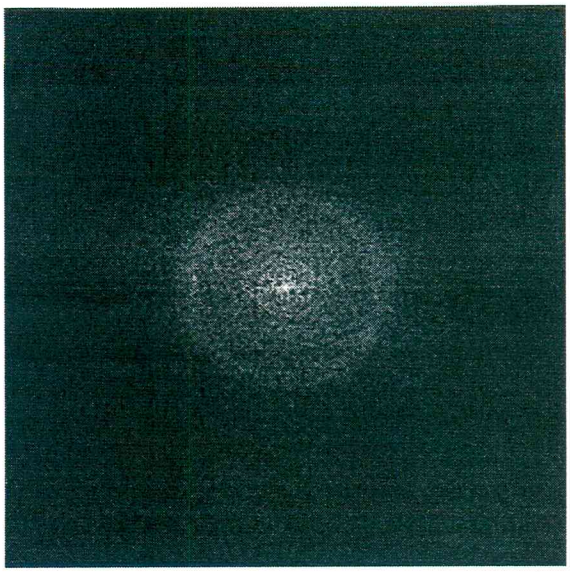

FIG. 4. FFT TEM image of the sample displaying Fig. 3 indicates an amorphous W_2N phase.

275 °C, as shown in Fig. 2(a). Alternatively, films grown at substrate temperatures above 275 °C exhibited XRD reflections that are consistent with the JCPDS PDF of a W_2N reference pattern, as shown in Fig. 2(b). The XRD findings are thus in agreement with the XPS data in terms of the formation of a W_2N phase.

Further microstructural investigations of the MOCVD-grown W_2N films were performed by TEM using a JEOL 2010F field emission electron microscope operating at 200 kV primary energy beam. TEM was performed on a JEOL 2010F system operating at 200 keV. Samples were tilted during TEM imaging so that the $\langle 110 \rangle$ zone axis of the silicon substrate was normal to the incident electron beam. The fast Fourier transform (FFT) method was applied to obtain diffraction patters from high-resolution bright field images when the selected area electron diffraction spot size exceeded the size of the area of interest. In this respect, Fig. 3

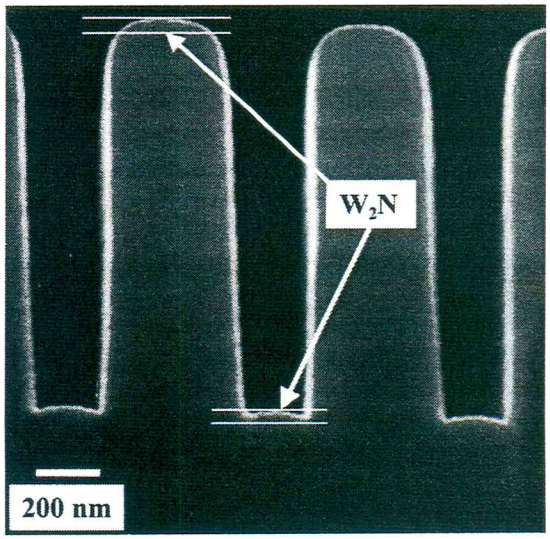

FIG. 5. Typical RBS spectrum of a MOCVD W_2N film.

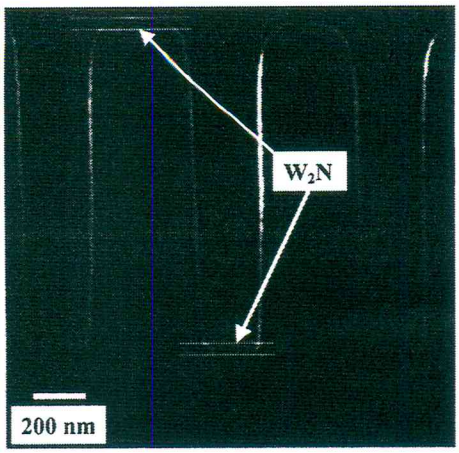

FIG. 6. Typical CS–SEM of MOCVD W_2N in nominal 0.25 μm trench structures.

displays a typical cross-section TEM bright field image of a W_2N film deposited at 200 °C. As can be seen, TEM confirmed our XRD data in terms of the amorphicity of 30-nm-thick W_2N films. This result is also supported by FFT analyses as exhibited in Fig. 4, which yielded a pattern that is characteristic of amorphous structures, namely, a continuous diffuse ring with no diffraction spots.

RBS was also performed to investigate the presence of any heavy element contaminants. A 2 MeV He^{2+} beam was used for the RBS measurements, and the resulting data was calibrated using bulk gold and carbon samples. No heavy element contaminants were detected by RBS, as shown in Fig. 5 for a typical RBS spectrum of a MOCVD W_2N sample.

W_2N conformality was studied using CS–SEM. CS–SEM was carried out on a Zeiss DSM940 microscope, employing a 20 keV primary electron beam and a beam current of 3.0 mA. Images taken by CS–SEM show step coverage of W_2N films to be better than 90% in nominal 0.25 μm trench structures, as demonstrated in the CS–SEM displayed in Fig. 6. In this case, step coverage was defined as the ratio of film thickness at the bottom of the structure to that in the field.

In summary, a low temperature MOCVD process has been identified for the formation of tungsten nitride films for potential applications as diffusion barrier in emerging copper-based metallization schemes. The process exploits the reaction of the nonfluorinated tungsten source tungsten hexacarbonyl, $W(CO)_6$, with H_2 and NH_3 to produce W_2N films within a wide process window, including substrate temperatures in the range 200 and 350 °C, $W(CO)_6$ flow rate of 1–20 sccm, reactor pressure of 0.2–0.5 Torr, and NH_3 flow rates of 100–500 sccm. Microstructural and microchemical analyses indicated that the tungsten nitride films consisted predominantly of a W_2N phase, with carbon and oxygen contamination $\leq$5 at. %, even at the lowest deposition temperature of 200 °C. Films deposited below 275 °C were amorphous, while those deposited between 275 and 350 °C were polycrystalline. Resistivities as low as 123 $\mu\Omega$ cm were achieved for 50-nm-thick films, with corresponding step coverage being higher than 90% in nominal 0.25 μm trench structures with aspect ratio of 4:1. These results indicate that the MOCVD route to W_2N using the nonfluorinated source $W(CO)_6$ could provide a viable alternative to inorganic CVD from WF_6 and NH_3, especially in terms of potential elimination of transport and handling concerns attributed to the high reactivity of the fluorinated WF_6 source, and reliability issues pertaining to the possible inclusion of fluorine, a fast diffuser in Cu in the WF_6-based CVD process.

The authors would like to acknowledge the Semiconductor Research Corporation (SRC) Center for Advanced Interconnect Science and Technology (CAIST) and the New York State Center for Advanced Thin Film Technology (CAT) for their support of the work presented herein.

[1]*The National Technology Roadmap for Semiconductors* (Semiconductor Industry Association, San Jose, CA, 1997), p. 99.
[2]M. Takeyama, A. Noya, T. Sase, and A. Ohta, J. Vac. Sci. Technol. B **14**, 674 (1996).
[3]M. Uekubo, T. Oku, K. Nii, M. Murakami, K. Takahiro, S. Yamaguchi, T. Nakano, and T. Ohta, Thin Solid Films **286**, 170 (1996).
[4]K. Nakajima, Y. Akasaka, K. Miyano, M. Takahashi, S. Suehiro, and K. Suguro, Appl. Surf. Sci. **117/118**, 312 (1997).
[5]B. Park *et al.*, J. Electron. Mater. **26**, 1 (1997).
[6]S. Marcus and R. Foster, Thin Solid Films **236**, 330 (1993).
[7]M. H. Tsai, S. C. Sun, H. T. Chiu, and S. H. Chuang, Appl. Phys. Lett. **68**, 1412 (1996).
[8]M. Takeyama and A. Noya, Jpn. J. Appl. Phys., Part 1 **36**, 2261 (1997).